

RESEARCH ARTICLE

# MicroRNA-124-3p alleviates repetitive bleomycin-induced idiopathic pulmonary fibrosis in mouse by repressing Wnt/ $\beta$ -catenin signaling component AXIN1

Dharma Jaggi, Kavita Aggarwal and Lavanya Goyal\*

Tezpur University, Institutional Biotech Hub, Napaam, Tezpur, Assam, India

## Abstract

**Background:** MicroRNA (miR)-124-3p is a crucial player in the transforming growth factor  $\beta$ 1-induced in vitro fibrogenic differentiation of mesenchymal stem cells. In the current study, we aimed to further verify the in vivo role of miR-124-3p in a mouse model of idiopathic pulmonary fibrosis (IPF).

**Methods:** Mouse IPF model was established using repetitive intratracheal bleomycin (BLM) dosing, followed by in vivo delivery of miR-124-3p. Masson's trichrome staining, hematoxylin-eosin (H&E), and modified Ashcroft score were performed on lung tissues to assess extent of pulmonary fibrosis. Collagen deposition was examined using hydroxyproline assay. Inflammatory cell counts were evaluated in the bronchoalveolar lavage (BAL) fluid. Terminal deoxynucleotidyl transferase dUTP nick end labeling (TUNEL) assay was performed to assess apoptosis in lung tissues.

**Results:** Repetitive BLM injection induced elevated fibrosis score and collagen deposition, elevated numbers of inflammatory cells in the BAL fluid, and promoted in lung tissues of mice. MiR-124-3p, to a considerable extent, reversed the BLM-induced IPF symptoms in terms of fibrosis score and collagen deposition in the lung tissues, reduced the BLM-elevated inflammatory cells in the BAL fluid and the percentage of BLM-induced apoptotic cells in lung tissues. AXIN1, a pivotal component in Wnt signaling, was also significantly inhibited by miR-124-3p in the experimental mice.

**Conclusion:** MiR-124-3p serves as a therapeutic target in the mouse model of IPF by repressing Wnt/ $\beta$ -catenin signaling component AXIN1 and holds great clinical potential in molecular therapies to treat human IPF patients.

**Keywords:** idiopathic pulmonary fibrosis; Wnt/ $\beta$ -catenin signaling; bleomycin; microRNA; C57BL/6 mouse

Received: 6 September 2023; Revised: 11 September 2023; Accepted: 13 September 2023; Published: 16 October 2023

Idiopathic pulmonary fibrosis (IPF) is a serious progressive and chronic condition affecting the lung, and in turn respiratory functions, without clear etiology. Five-year survival of IPF patients is less than 50% (1), primarily due to the lack of understanding regarding IPF pathogenesis, inadequate treatment options, late diagnosis, and poor prognosis (2). A number of novel therapeutic targets have been identified over the years, a few of which currently are in the process of clinical trials. Nonetheless, there still lacks effective approved treatments. Hence, it is of great importance to gather better insights into the mechanisms underlying IPF in order to explore new therapeutic possibilities.

Both genetic and non-genetic risk factors, such as infection, aging, and smoking, are believed to contribute

to the pathogenesis of IPF. Combined, these factors may lead to damaged alveolar epithelial cells and fibroblasts, deposition of extracellular matrix, abnormal wound healing, and formation of fibroblastic/myofibroblastic foci (3–5), eventually giving rise to impaired respiratory functions and gas exchange, as well as dyspnea. During such process, mesenchymal stem cells (MSCs) are critically involved (6). MSCs, a type of pluripotent stem cells, reside in the bone marrow as well as a variety of organs such as the liver, brain, and lung. Such tissue-resident MSCs are capable of differentiating into progenitor cells that are organ-specific. Accumulating data suggest that lung-resident MSCs (LR-MSCs) are involved in the microvascular remodeling in the lung acting as multipotent vascular precursors (7). Further, LR-MSCs could

reportedly differentiate into alveolar epithelial type II cells (8) and are engaged in the wound healing of the lung (9), which may also result in pulmonary disorders under certain circumstances (6).

The importance of Wnt/ $\beta$ -catenin signaling has been frequently implicated in lung diseases. Abnormal activation of this signaling pathway may result in lung cancer and pulmonary fibrosis (10, 11). Recent investigations consistently indicate that MSC differentiation and self-renewal are under the control of Wnt/ $\beta$ -catenin signaling. Thus it is plausible that Wnt signaling could be involved in pulmonary diseases through regulation of MSCs. Recently, we have also reported that microRNA (miRNA, miR)-124-3p could regulate transforming growth factor (TGF)- $\beta$ 1-elicited LR-MSC differentiation to myofibroblast through inhibition of Wnt/ $\beta$ -catenin (12).

## Materials and methods

### Mouse IPF model

Mouse IPF model in the current study was adapted from a repetitive intratracheal bleomycin (BLM) dosing method as previously described (13). Male 8-week-old C57BL/6J mice were purchased from Shanghai Laboratory Animal Center (Shanghai, China). BLM solution was obtained by dissolving sterile BLM sulfate powder (Teva Parenteral Medicines, Irvine, CA) in sterile standard saline. Intratracheal injection of BLM was conducted at the dosage of 0.04 units in 100  $\mu$ L sterile saline on a biweekly basis for a period of 16 weeks. For the intubation procedure, animals were deeply sedated through inhaled isoflurane and then suspended by the front teeth on an angled fiberglass stand. In order to obtain a clear view of the trachea, the tongue was gently lifted using forceps and the palate was lifted using a small scoop, similar to a Miller blade on a laryngoscope. A 26-French angiocatheter was inserted into the trachea, followed by the administration of 100  $\mu$ L of BLM solution. Animals were continually monitored after the procedure to ensure proper recovery. Mice in the sham group received identical procedure with 100  $\mu$ L of sterile saline without BLM.

### In vivo delivery of miR-124-3p

MiR-124-3p and negative control (miR-NC) were formulated with MaxSuppressor In Vivo RNA-LANCER II (Bioo Scientific) according to the manufacturer's instructions. At week 16 into the repetitive BLM injection, the mice were also injected i.p. at 2  $\mu$ g/g body weight of either miR-124-3p or miR-NC. Seven days later, all mice were euthanized and lungs were harvested.

### Hematoxylin-eosin staining and Masson's trichrome staining

Harvested left lung samples fixed using 4% paraformaldehyde were paraffin-embedded for preparation of sections

at 2  $\mu$ m thickness, which were then stained using hematoxylin and eosin. In order to evaluate lung fibrosis, Masson's trichrome staining was conducted. On each section, five non-overlapping microscopic fields that contained most severe injuries of lung parenchyma were examined. Histological examination of lung fibrosis was quantified with the use of the modified Ashcroft score (14). The fibrosis severity in each field of a lung specimen was recorded as a score of 0–8 by a pathologist blind to group assignment, and the overall severity of any given lung section was calculated as the mean score of the five fields.

### Hydroxyproline assay

Homogenates of right lung tissues were generated and examined for hydroxyproline content in accordance to the provided guides (Wuhan EIAab Science Co., Ltd., China). In brief, homogenized samples were stored at  $-20^{\circ}\text{C}$  overnight. After two cycles of 'freeze and thaw', the homogenates were centrifuged at 5000 g for 5 min. The supernatants were then collected and the absorbance at 450 nm was measured to determine the abundance of hydroxyproline content (ng hydroxyproline/mg protein).

### Bronchoalveolar lavage fluid analysis

Bronchoalveolar lavage (BAL) was collected through a 20-gauge needle inserted into the trachea. Sterile phosphate buffered saline (PBS, 0.6 mL each time, three times) was slowly delivered into the lung through the trachea, then BAL fluid was harvested, and subjected to centrifugation at 400 g for 10 min. For each sample, around 30,000 cells were loaded onto a glass slide for cell counting under light microscopy using Giemsa stain.

### Terminal deoxynucleotidyl transferase dUTP nick end labeling assay

Terminal deoxynucleotidyl transferase dUTP nick end labeling (TUNEL) assay was conducted with the usage of a commercially available kit according to the provided protocol (In Situ Apoptosis Detection Kit, Millipore, MA, USA). In brief, lung samples fixed using 10% neutral buffered formaldehyde were paraffin-embedded and sectioned at 4–5  $\mu$ m thickness. Counterstain was carried out using Mayer's hematoxylin. For each specimen, TUNEL-positive cells on 10 consecutive, non-overlapping high-magnification fields were counted. The mean number of cells with TUNEL-positive nuclei from these fields was regarded as the apoptotic score for each specimen.

### Quantitative real-time polymerase chain reaction

Total RNA was extracted with the use of TRIzol reagent (Invitrogen, Carlsbad, CA). Then, 2  $\mu$ g of total RNA was reverse transcribed into cDNA using a specific stem-loop primer (Guangzhou RiboBio Co., Ltd.). Quantitative

polymerase chain reaction (PCR) was performed on the ABI7000 Real-Time PCR system (Applied Biosystems; Thermo Fisher Scientific, Inc.) using SYBR Green master mix. Primers used in this study were miR-124-3p forward 5'-AGG CAC GCG GTG A-3', reverse 5'-TCC AGT TTT TTT TTT TTT TTG GCA-3'; AXIN1 forward 5'-ACG GTA CAA CGA AG CAG AGA GCT-3', reverse 5'-CGG ATC TCC TTT GGC ATT CGG TAA-3'; GAPDH forward 5'-AAC TTT GGC ATT GTG GAA GG-3', reverse 5'-ACA CAT TGG GGG TAG GAA CA-3'.

#### Western Blotting

The total protein was extracted from samples of lung tissues using standard RIPA buffer (Cell Signaling Technology Inc., Danvers, MA). Proteins of equal amount were subjected to 10% sodium dodecyl sulfate polyacrylamide gel electrophoresis (SDS-PAGE) and then transferred onto polyvinylidene difluoride membranes (Bio-Rad) followed by blocking using 5% non-fat milk. All primary antibodies, namely AXIN1 and GAPDH as the loading control, were obtained from Abcam (Cambridge, MA,) and used at 1:1000 dilution. Membranes were then incubated with horseradish peroxidase-conjugated goat anti-rabbit/mouse IgG

(Boster, Wuhan, China). The resulted immunoreactivity was determined on an Odyssey Scanning System (LI-COR, Inc., Lincoln, NE).

#### Statistical analysis

All data were presented as mean  $\pm$  standard deviation (SD). SPSS version 19.0 (IBM SPSS, Amronk, NY, USA) was used for statistical analysis. Statistical differences were determined using one-way analysis of variance (ANOVA) analysis or the Student's t-test. Values of  $P < 0.05$  were regarded to indicate statistical significance.

## Results

#### Repetitive BLM induces IPF symptoms in model mice

To establish a repetitive BLM injury model, we employed direct laryngeal intubation to administer BLM on a biweekly basis for eight doses (see Materials and Methods). One week after the last dose of BLM or vehicle control, BLM and sham mice were euthanized and lungs were harvested.

Histological examination of lung tissues from mice receiving repetitive BLM administrations using trichrome blue collagen staining revealed extensive extracellular matrix deposition and fibrosis (Fig. 1a). On the basis of

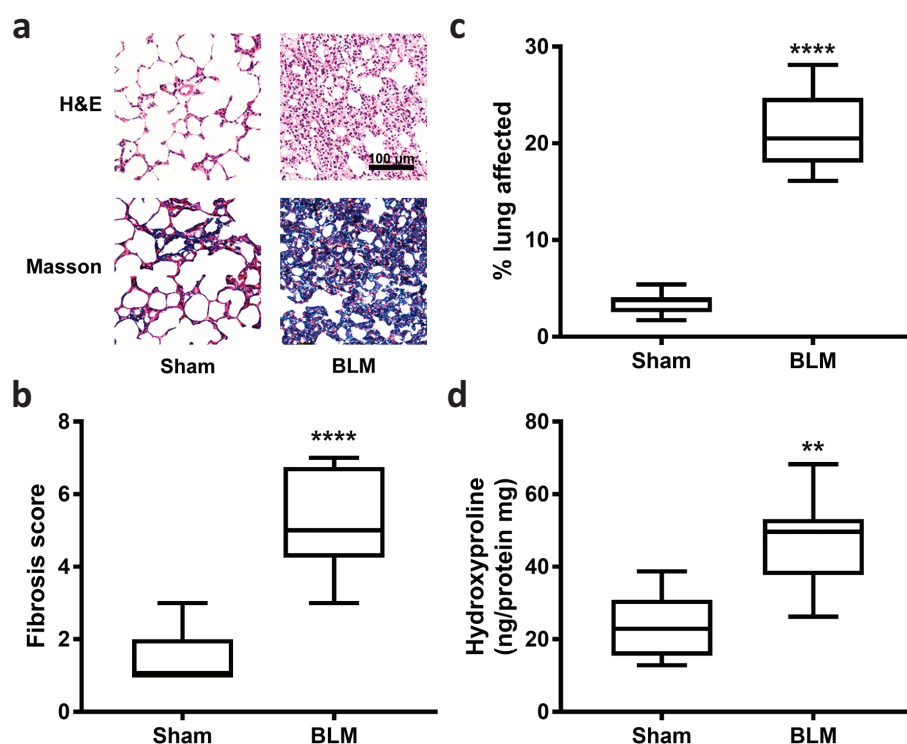


**Fig. 1.** Repetitive bleomycin (BLM) treatment induces severe idiopathic pulmonary fibrosis (IPF). (a) Representative lung sections stained with hematoxylin-eosin (H&E) (upper row) and Masson's trichrome staining (lower row) in sham and BLM group mice. Scale bar, 100  $\mu$ m. (b) Fibrosis scoring using the modified Ashcroft score in sham and BLM group mice. (c) Morphometry measurements of lung sections showing percentage of lung tissue affected by fibrosis in sham and BLM group mice. (d) Collagen deposition was assessed by hydroxyproline measurement in sham and BLM group mice. Data are presented as median (min, max,  $N = 8$  each group), \*\* $P < 0.01$ , \*\*\*\* $P < 0.0001$ , sham versus BLM.

such prominent histological alterations, we compared the extent of lung fibrosis between the sham and BLM groups of mice, using quantitative evaluations. Trichrome-stained lung specimens were assessed on seriousness of fibrosis in a blinded manner using modified Ashcroft score with a 0–8 scale (14). It turned out that fibrosis score of BLM group was significantly higher than that of the sham mice (Fig. 1b). In addition, a remarkably higher percentage of lung samples exhibited fibrotic alterations in the mice receiving repetitive BLM injection than mice receiving sham injection (Fig. 1c). Next, collagen deposition was evaluated through measurement of hydroxyproline content in lung tissues (ng hydroxyproline/mg protein), which was also found to be much higher in the BLM group than sham group (Fig. 1d).

Moreover, as an indication of inflammatory response in the lung, we assessed number of inflammatory cells in the BAL fluid in both groups of mice. Repetitive exposure to BLM increased inflammatory cells of all types (Fig. 2a), including macrophages (Fig. 2b), neutrophils (Fig. 2c), and lymphocytes (Fig. 2d), with macrophage being the most common type.

We also evaluated *in situ* apoptosis by TUNEL staining and found that the number of apoptotic cells was markedly increased in the BLM group compared to the sham group (Fig. 3a and b).

#### *In vivo* delivery of miR-124-3p reverses IPF symptoms in repetitive BLM model mice

In the current study, we utilized an miRNA *in vivo* delivery system, which efficiently increased the expression of miR-124-3p (Fig. 4a) but inhibited the expression of both AXIN1 mRNA (Fig. 4b) and protein (Fig. 4c), which is shown to be a specific target of miR-124-3p (12).

With the successful *in vivo* miR-124-3p expression, we continued to examine the *in vivo* effect of miR-124-3p on repetitive BLM-induced IPF mouse model. The extensive fibrosis and extracellular matrix deposition earlier observed in BLM mice were greatly alleviated following miR-124-3p *in vivo* expression (Fig. 5a). Quantitative fibrosis score was consistent with the histological evaluations, showing that miR-124-3p in BLM mice could, although incompletely, reduce the score by a great extent (Fig. 5b). Percentage of lung with fibrosis and collagen deposition followed the same trend as fibrosis score in the three experimental groups as well (Fig. 5c and d). These results strongly demonstrated the alleviating effect of miR-124-3p *in vivo* against repetitive BLM-induced lung fibrosis in mice.

Similarly, inflammatory cell counting was performed in all three groups of experimental mice. As expected, introducing miR-124-3p expression in the BLM-inflicted mice could significantly reduce the numbers of all major types of inflammatory cells in the BAL fluid (Fig. 6a–d), further

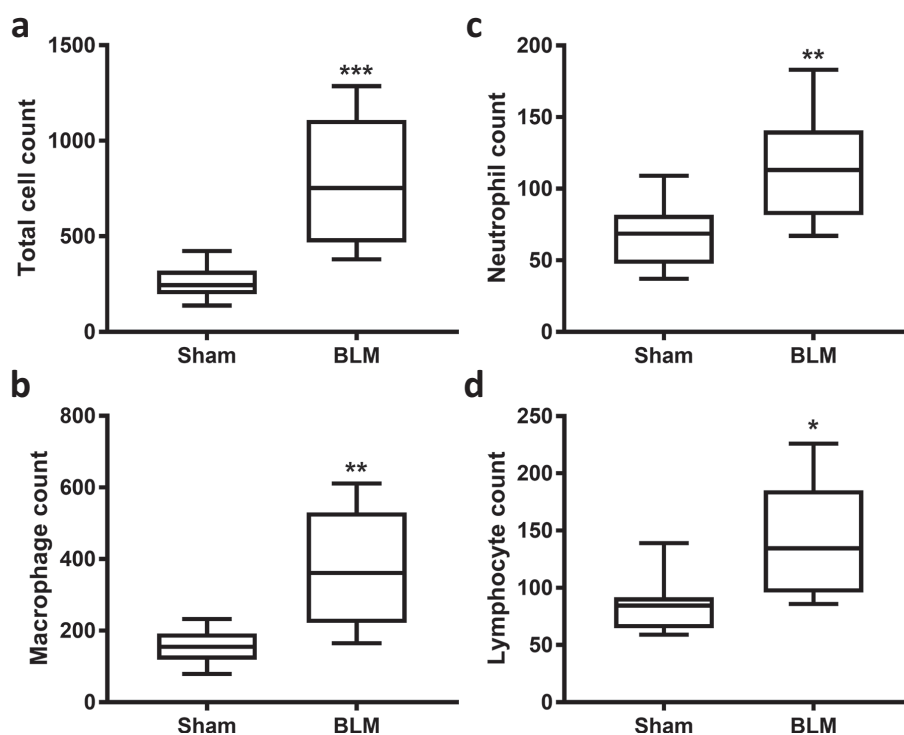


**Fig. 2.** Repetitive bleomycin (BLM) treatment elevates number of inflammatory cells in bronchoalveolar lavage (BAL) fluid. (a) The total cell count, (b) macrophage count, (c) neutrophil count, and (d) lymphocyte count in BAL fluid in sham and BLM group mice. Data are presented as median (min, max,  $N = 8$  each group), \* $P < 0.05$ , \*\* $P < 0.01$ , \*\*\* $P < 0.001$ , sham versus BLM.

supporting the benefit of miR-124-3p against inflammatory response in IPF model mice. Last but not least, as indicated by TUNEL staining assay in lung tissues from all groups, the number of apoptotic cells was also significantly repressed in the BLM group receiving miR-124-3p delivery (Fig. 7a and b).

## Discussion

Establishing appropriate animal models of human diseases is the prerequisite of any preclinical investigations. In this context, the C57BL/6J mice have been used as the primary model animal for IPF for their high susceptibility to lung injuries following intratracheal BLM administrations (15, 16). On the other hand, the SV129 or BALB/c strains exhibit resistance to BLM-elicited pulmonary fibrosis, likely as a result of altered TGF- $\beta$  expression (16). This phenomenon echoes the genetic susceptibility and other potential risk factors for inducing fibrosis in end organs after BLM exposures observed in humans. Investigations on BLM-elicited pulmonary fibrosis have mainly used young male mice between 8 and 12 weeks (17–19).

Another important aspect in terms of our current C57BL/6J mouse IPF model was a repetitive dosing of BLM rather than a single dose. Most reports assessing therapeutic interventions did not use repetitive administrations;

rather, a single dose of intratracheal BLM is often used and immediately followed by the application of the agent under investigation (20–23). To our knowledge, only two investigations so far have examined injuries caused by repetitive BLM exposures (13, 24, 25). Lee et al. employed biweekly intratracheal administrations of 0.04 U BLM for a total period of 4 months in young mice (24). In mice with repeated administrations, infiltration of the perialveolar ducts by inflammatory cells, hyperplasia of cuboidal alveolar epithelial cells and club cells (Clara cells), enlarged alveoli, septal thickening, and extensive fibrosis were observed (24). In addition, potential therapeutic agents are often applied within 1–7 days post exposure to BLM, giving rise to the belief that the therapy may exert beneficial effects predominantly by preventing inflammatory events instead of reversing fibrosis, hence greatly hindering the translation to human IPF (26). Latest reports have started to investigate drugs administered after the initial week (27, 28).

Therefore based on the earlier studies, in our current experimental design, we employed 8-week-old male C57BL/6J mice and administered them with repetitive BLM dosing, followed by *in vivo* delivery of miR-124 after 7 days. These mice almost precisely recapitulated symptoms of human IPF. First of all, repetitive BLM injection induced severe IPF, evidenced by elevated fibrosis score and collagen deposition. In addition, numbers of inflammatory cells in the BAL fluid, including macrophages, neutrophils, and lymphocytes, have been greatly increased by repetitive BLM injection. Moreover, elevated apoptosis was also observed in lung tissues of mice receiving repetitive BLM injection.

MiRNAs are a class of small noncoding RNAs that bind to the 3' (untranslated region) UTR of target mRNAs, leading to repressed protein expression primarily through destabilization of the target mRNAs and/or inhibition of translation. MiRNAs exert critical functions in numerous biological processes including IPF (29) and have recently been particularly implicated in TGF- $\beta$  signaling pathway-mediated IPF (30). In our current study, we sorted to verify the *in vitro* observed role of miR-124-3p in the established mouse IPF model *in vivo*. We first utilized an miRNA *in vivo* delivery system,

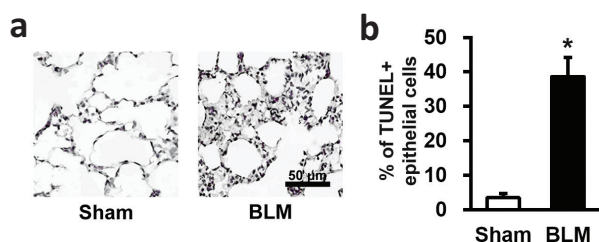


**Fig. 3.** Repetitive bleomycin (BLM) treatment increases apoptotic cells in lung tissues. (a) Representative images of TUNEL staining from lung sections in sham and BLM group mice. Scale bar, 50  $\mu$ m. (b) Quantitative analysis of TUNEL-positive epithelial cells in the lung tissue of sham and BLM group mice. Data are presented as mean  $\pm$  SD ( $N = 8$  each group), \* $P < 0.05$ , sham versus BLM.

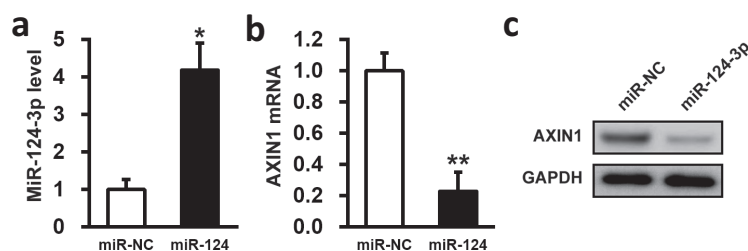


**Fig. 4.** Effect of *in vivo* delivery of miR-124-3p suppresses endogenous AXIN1 expression. Levels of (a) miR-124-3p, (b) AXIN1 mRNA, and (c) AXIN1 protein were analyzed in lung tissues of mice receiving *in vivo* delivery of either miR-negative control (miR-NC) or miR-124-3p mimic (miR-124). Data are presented as mean  $\pm$  SD ( $N = 6$  each group), \* $P < 0.05$ , \*\* $P < 0.01$ , miR-NC versus miR-124.

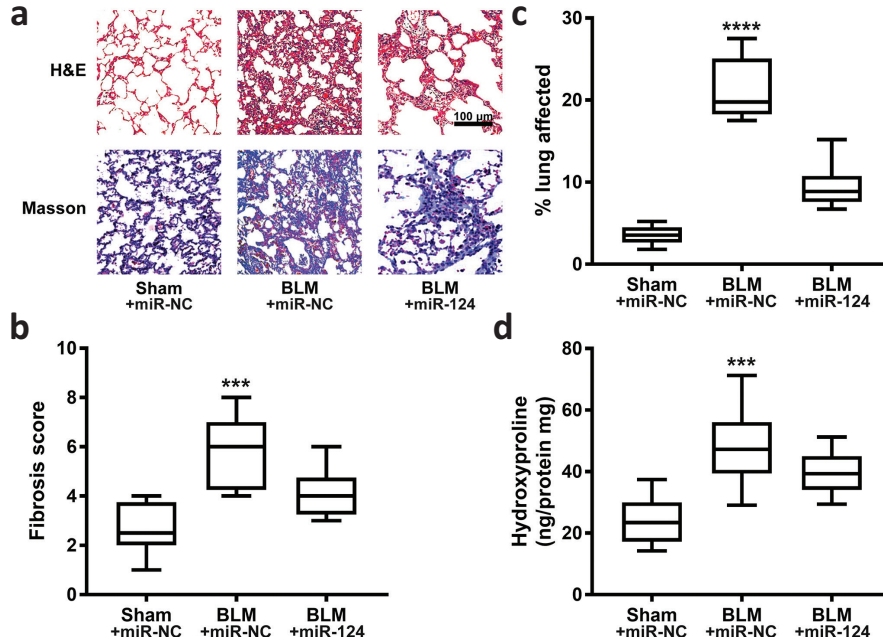


**Fig. 5.** MiR-124-3p reverses bleomycin (BLM)-induced idiopathic pulmonary fibrosis (IPF). (a) Representative lung sections stained with hematoxylin-eosin (H&E) (upper row) and Masson's trichrome staining (lower row) in sham+miR-NC, BLM+miR-NC and BLM+miR-124-3p mimic (miR-124) group mice. Scale bar, 100 μm. (b) Fibrosis scoring using the modified Ashcroft score in sham+miR-NC, BLM+miR-NC, and BLM+miR-124 group mice. (c) Morphometry measurements of lung sections showing percentage of lung tissue affected by fibrosis in sham+miR-NC, BLM+miR-NC, and BLM+miR-124 group mice. (d) Collagen deposition was assessed by hydroxyproline measurement in sham+miR-NC, BLM+miR-NC, and BLM+miR-124 group mice. Data are presented as median (min, max,  $N = 8$  each group), \*\*\* $P < 0.001$ , \*\*\*\* $P < 0.0001$ , BLM+miR-NC versus both sham+miR-NC and BLM+miR-124.

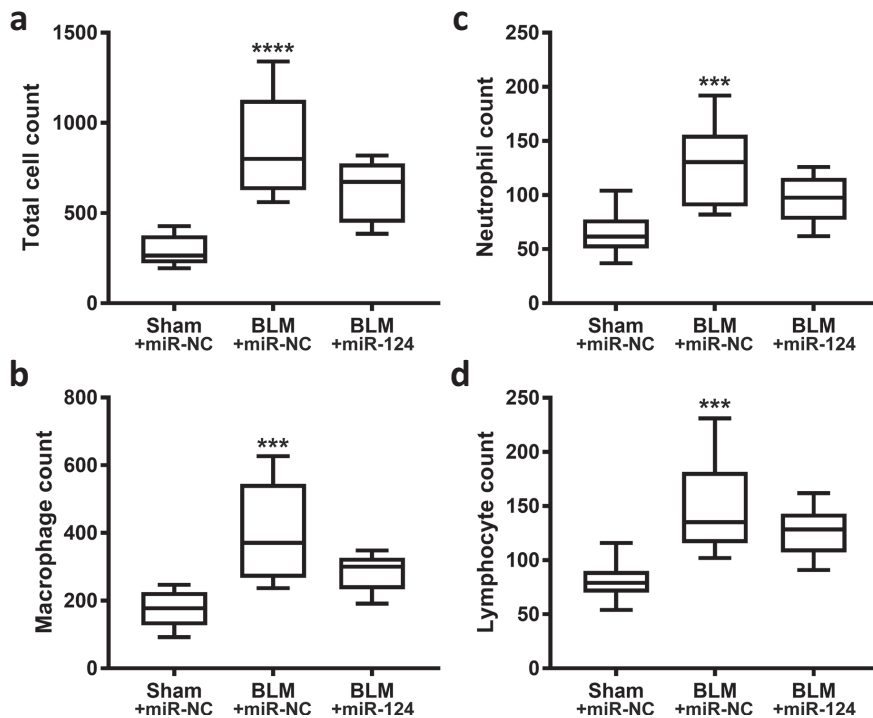


**Fig. 6.** MiR-124-3p reverses bleomycin (BLM)-elevated inflammatory cells in bronchoalveolar lavage (BAL) fluid. (a) The total cell count, (b) macrophage count, (c) neutrophil count, and (d) lymphocyte count in BAL fluid in sham+miR-NC, BLM+miR-NC, and BLM+miR-124-3p mimic (miR-124) group mice. Data are presented as median (min, max,  $N = 8$  each group), \*\*\* $P < 0.001$ , \*\*\*\* $P < 0.0001$ , BLM+miR-NC versus both sham+miR-NC and BLM+miR-124.

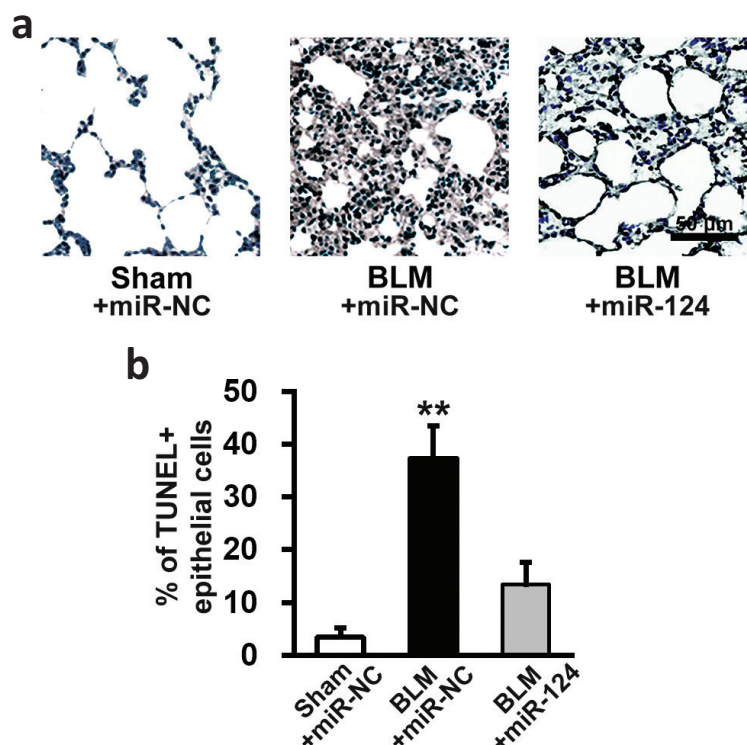


**Fig. 7.** MiR-124-3p reverses bleomycin (BLM)-induced apoptotic cells in lung tissues. (a) Representative images of TUNEL staining from lung sections in sham+miR-NC, BLM+miR-NC, and BLM+miR-124-3p mimic (miR-124) group mice. Scale bar, 50  $\mu$ m. (b) Quantitative analysis of TUNEL-positive epithelial cells in the lung tissue of sham+miR-NC, BLM+miR-NC, and BLM+miR-124 group mice. Data are presented as mean  $\pm$  SD ( $N = 8$  each group), \*\* $P < 0.01$ , BLM+miR-NC versus both sham+miR-NC and BLM+miR-124.

which efficiently increased the expression of miR-124-3p whereas inhibited expression of AXIN1, which is shown to be a specific target of miR-124-3p (12) in the experimental mice. Next, miR-124-3p was delivered in the IPF model mice, followed by examination of IPF symptoms. Surprisingly, we found that miR-124-3p reversed, to a considerable extent, the BLM-induced IPF symptoms in terms of fibrosis score and collagen deposition in the lung tissues. Besides, the elevated inflammatory cells in the BAL fluid following repetitive BLM injection were also largely reduced by miR-124-3p. Lastly, miR-124-3p also reduced the percentage of BLM-induced apoptotic cells in lung tissues. Importantly, AXIN1, a critical component in Wnt signaling, was also significantly repressed by miR-124-3p in the experimental mice. Wnt/ $\beta$ -catenin signaling plays key roles in various processes within the context of IPF. In IPF tissues,  $\beta$ -catenin was enriched in the nucleus, indicating that Wnt signaling is activated (31). Sustained Wnt activation was believed to be involved in the proliferative myofibroblast lesions and to be engaged in the lung fibrosis (32). Further, Wnt signaling reportedly regulates LR-MSCs differentiation (7, 33).

### Conclusion

To conclude, our current study is the first instance to date, to present in vivo evidences supporting the

crucial role of miR-124-3p as a therapeutic target in the mouse model of IPF by repressing Wnt/ $\beta$ -catenin signaling component AXIN1, and holds great clinical potential in molecular therapies to treat human IPF patients.

### Conflict of interest and funding

The authors declare that they have no competing interest. No funding is derived for this work.

### References

1. Caminati A, Cassandro R, Torre O, Harari S. Severe idiopathic pulmonary fibrosis: what can be done? *Eur Respir Rev* 2017; 26(145): 170047. doi: 10.1183/16000617.0047-2017
2. Kolb M, Bonella F, Wollin L. Therapeutic targets in idiopathic pulmonary fibrosis. *Respir Med* 2017; 131: 49–57. doi: 10.1016/j.rmed.2017.07.062
3. Selman M, King TE, Pardo A. Idiopathic pulmonary fibrosis: prevailing and evolving hypotheses about its pathogenesis and implications for therapy. *Ann Intern Med* 2001; 134(2): 136–51. doi: 10.7326/0003-4819-134-2-200101160-00015
4. Selman M, Pardo A, Barrera L, Estrada A, Watson SR, Wilson K, et al. Gene expression profiles distinguish idiopathic pulmonary fibrosis from hypersensitivity pneumonitis. *Am J Respir Crit Care Med* 2006; 173(2): 188–98. doi: 10.1164/rccm.200504-644OC

5. Thannickal VJ, Toews GB, White ES, Lynch Iii JP, Martinez FJ. Mechanisms of pulmonary fibrosis. *Annu Rev Med* 2004; 55: 395–417. doi: 10.1146/annurev.med.55.091902.103810
6. Tzouveleki A, Koliakos G, Ntoliou P, Baira I, Bouros E, Oikonomou A, et al. Stem cell therapy for idiopathic pulmonary fibrosis: a protocol proposal. *J Transl Med* 2011; 9(1): 182. doi: 10.1186/1479-5876-9-182
7. Chow K, Fessel JP, Kaorihida-Stansbury, Schmidt EP, Gaskill C, Alvarez D, et al. Dysfunctional resident lung mesenchymal stem cells contribute to pulmonary microvascular remodeling. *Pulm Circ* 2013; 3(1): 31–49. doi: 10.4103/2045-8932.109912
8. Gong X, Sun Z, Cui D, Xu X, Zhu H, Wang L, et al. Isolation and characterization of lung resident mesenchymal stem cells capable of differentiating into alveolar epithelial type II cells. *Cell Biol Int* 2014; 38(4): 405–11. doi: 10.1002/cbin.10240
9. Jones E, McGonagle D. Human bone marrow mesenchymal stem cells in vivo. *Rheumatology* 2007; 47(2): 126–31. doi: 10.1093/rheumatology/kem206
10. Königshoff M, Balsara N, Pfaff E-M, Kramer M, Chrobak I, Seeger W, et al. Functional Wnt signaling is increased in idiopathic pulmonary fibrosis. *PLoS One* 2008; 3(5): e2142. doi: 10.1371/journal.pone.0002142
11. Uematsu K, He B, You L, Xu Z, McCormick F, Jablons DM. Activation of the Wnt pathway in non small cell lung cancer: evidence of dishevelled overexpression. *Oncogene* 2003; 22(46): 7218. doi: 10.1038/sj.onc.1206817
12. Lu Y, Zhang T, Shan S, Wang S, Bian W, Ren T, et al. MiR-124 regulates transforming growth factor-beta1 induced differentiation of lung resident mesenchymal stem cells to myofibroblast by repressing Wnt/beta-catenin signaling. *Dev Biol* 2019; 449(2): 115–21. doi: 10.1016/j.ydbio.2019.02.010
13. Degryse AL, Tanjore H, Xu XC, Polosukhin VV, Jones BR, McMahon FB, et al. Repetitive intratracheal bleomycin models several features of idiopathic pulmonary fibrosis. *Am J Physiol Lung Cell Mol Physiol* 2010; 299(4): L442–52. doi: 10.1152/ajplung.00026.2010
14. Hubner RH, Gitter W, El Mokhtari NE, Mathiak M, Both M, Bolte H, et al. Standardized quantification of pulmonary fibrosis in histological samples. *BioTechniques* 2008; 44(4): 507–11, 14–7. doi: 10.2144/000112729
15. Stefanov AN, Fox J, Depault F, Haston CK. Positional cloning reveals strain-dependent expression of Trim16 to alter susceptibility to bleomycin-induced pulmonary fibrosis in mice. *PLoS Genet* 2013; 9(1): e1003203. doi: 10.1371/journal.pgen.1003203
16. Hoyt DG, Lazo JS. Alterations in pulmonary mRNA encoding procollagens, fibronectin and transforming growth factor-beta precede bleomycin-induced pulmonary fibrosis in mice. *J Pharmacol Exp Ther* 1988; 246(2): 765–71.
17. Peng R, Sridhar S, Tyagi G, Phillips JE, Garrido R, Harris P, et al. Bleomycin induces molecular changes directly relevant to idiopathic pulmonary fibrosis: a model for 'active' disease. *PLoS One* 2013; 8(4): e59348. doi: 10.1371/journal.pone.0059348
18. Izbicki G, Segel MJ, Christensen TG, Conner MW, Breuer R. Time course of bleomycin-induced lung fibrosis. *Int J Exp Pathol* 2002; 83(3): 111–9. doi: 10.1046/j.1365-2613.2002.00220.x
19. Aguilar S, Scotton CJ, McNulty K, Nye E, Stamp G, Laurent G, et al. Bone marrow stem cells expressing keratinocyte growth factor via an inducible lentivirus protects against bleomycin-induced pulmonary fibrosis. *PLoS One* 2009; 4(11): e8013. doi: 10.1371/journal.pone.0008013
20. Ortiz LA, Gambelli F, McBride C, Gaupp D, Baddoo M, Kaminski N, et al. Mesenchymal stem cell engraftment in lung is enhanced in response to bleomycin exposure and ameliorates its fibrotic effects. *Proc Natl Acad Sci U S A* 2003; 100(14): 8407–11. doi: 10.1073/pnas.1432929100
21. Rojas M, Xu J, Woods CR, Mora AL, Spears W, Roman J, et al. Bone marrow-derived mesenchymal stem cells in repair of the injured lung. *Am J Respir Cell Mol Biol* 2005; 33(2): 145–52. doi: 10.1165/rcmb.2004-0330OC
22. Ortiz LA, Dutreil M, Fattman C, Pandey AC, Torres G, Go K, et al. Interleukin 1 receptor antagonist mediates the antiinflammatory and antifibrotic effect of mesenchymal stem cells during lung injury. *Proc Natl Acad Sci U S A* 2007; 104(26): 11002–7. doi: 10.1073/pnas.0704421104
23. Fokkett AM, Bazhanov N, Ti X, Tiblow A, Bartosh TJ, Prockop DJ. Phase-directed therapy: TSG-6 targeted to early inflammation improves bleomycin-injured lungs. *Am J Physiol Lung Cell Mol Physiol* 2014; 306(2): L120–31. doi: 10.1152/ajplung.00240.2013
24. Lee SH, Lee EJ, Lee SY, Kim JH, Shim JJ, Shin C, et al. The effect of adipose stem cell therapy on pulmonary fibrosis induced by repetitive intratracheal bleomycin in mice. *Exp Lung Res* 2014; 40(3): 117–25. doi: 10.3109/01902148.2014.881930
25. Moodley Y, Vaghjiani V, Chan J, Baltic S, Ryan M, Tchongue J, et al. Anti-inflammatory effects of adult stem cells in sustained lung injury: a comparative study. *PLoS One* 2013; 8(8): e69299. doi: 10.1371/journal.pone.0069299
26. Srouf N, Thebaud B. Mesenchymal stromal cells in animal bleomycin pulmonary fibrosis models: a systematic review. *Stem Cells Transl Med* 2015; 4(12): 1500–10. doi: 10.5966/sctm.2015-0121
27. Cross J, Stenton GR, Harwig C, Szabo C, Genovese T, Di Paola R, et al. AQX-1125, small molecule SHIP1 activator inhibits bleomycin-induced pulmonary fibrosis. *Br J Pharmacol* 2017; 174(18): 3045–57. doi: 10.1111/bph.13934
28. Tanaka KI, Niino T, Ishihara T, Takafuji A, Takayama T, Kanda Y, et al. Protective and therapeutic effect of felodipine against bleomycin-induced pulmonary fibrosis in mice. *Sci Rep* 2017; 7(1): 3439. doi: 10.1038/s41598-017-03676-y
29. Pandit KV, Milosevic J. MicroRNA regulatory networks in idiopathic pulmonary fibrosis. *Biochem Cell Biol* 2015; 93(2): 129–37. doi: 10.1139/bcb-2014-0101
30. Kang H. Role of MicroRNAs in TGF-beta signaling pathway-mediated pulmonary fibrosis. *Int J Mol Sci* 2017; 18(12): 2527. doi: 10.3390/ijms18122527
31. Chilosi M, Poletti V, Zamò A, Lestani M, Montagna L, Piccoli P, et al. Aberrant Wnt/beta-catenin pathway activation in idiopathic pulmonary fibrosis. *Am J Pathol* 2003; 162(5): 1495–502. doi: 10.1016/S0002-9440(10)64282-4
32. Königshoff M, Kramer M, Balsara N, Wilhelm J, Amarie OV, Jahn A, et al. WNT1-inducible signaling protein-1 mediates pulmonary fibrosis in mice and is upregulated in humans with idiopathic pulmonary fibrosis. *J Clin Invest* 2009; 119(4): 772–87. doi: 10.1172/JCI33950
33. Wang Y, Sun Z, Qiu X, Li Y, Qin J, Han X. Roles of Wnt/beta-catenin signaling in epithelial differentiation of mesenchymal stem cells. *Biochem Biophys Res Commun* 2009; 390(4): 1309–14. doi: 10.1016/j.bbrc.2009.10.143

---

**\*Lavanya Goyal**

Tezpur University,  
 Institutional Biotech Hub,  
 Napaam, Tezpur,  
 Assam 784028, India  
 Email: LavanyaGoyal55@outlook.com